IEEE Access
Multidisciplinary | Rapid Review | Open Access Journal

Received 27 October 2022, accepted 12 November 2022, date of publication 14 November 2022,
date of current version 21 November 2022.

Digital Object Identifier 10.1109/ACCESS.2022.3222406

RESEARCH ARTICLE

Novel Gaussian Acceleration Profile for Smooth Jerk-Bounded Trajectories

GONZALEZ-VILLAGOMEZ ESAU[1], RODRIGUEZ-DONATE CARLOS[1], (Member, IEEE), MATA-CHAVEZ RUTH IVONNE[1], CABAL-YEPEZ EDUARDO[1], (Member, IEEE), LOPEZ-HERNANDEZ JUAN MANUEL[1], AND PALILLERO-SANDOVAL OMAR[2]

[1]División de Ingenierías, Campus Irapuato-Salamanca, Departamento de Estudios Multidisciplinarios, Universidad de Guanajuato, Yuriria, Guanajuato 38944, Mexico
[2]Center for Research in Engineering and Applied Science (CIICAp), Institute for Research in Pure and Applied Science (IICBA), UAEM, Chamilpa, Cuernavaca 62209, Mexico

Corresponding author: Rodriguez-Donate Carlos (c.rodriguezdonate@ugto.mx)

This work was supported by the Consejo Nacional de Ciencia y Tecnología (CONACYT), México, under Scholarship 818467; and in part by Dirección de Apoyo a la Investigación y Posgrado de la Universidad de Guanajuato (DAIP-UG), Convocatoria Institucional de Investigación Científica 2022, under Project 118/2022.

ABSTRACT Industrial machines regularly work at their limits causing excessive long-term vibrations that deteriorate their movement, stability, and precision. In this sense, reference profiles are able to reduce the detrimental vibration effects by manipulating the machine motion dynamics using predefined movement trajectories. Most of the approaches for lessening damages due to long-term machine vibrations are based on polynomial functions with high computational complexity and high resources demand. Hence, in this work, an innovative acceleration outline based on a Gaussian function is proposed for machine motion trajectories. The introduced strategy simplifies the position-profile estimation that works as reference for restraining the machine movements through the parameters that define its motion dynamics; thus, a smooth and continuous jerk contour is produced, which reduces vibrations and improves the machine stability. Exhaustive computer-based and real-time experimental comparisons of the introduced scheme produces a significantly lower maximum jerk value than any of the others. The assessment of the presented approach was performed utilizing the software Matlab (R2020a) on a PC with an Intel Core i7-6500U microprocessor at 2.5 GHz, with 16 GB in RAM and a 64-bit operating system.

INDEX TERMS Acceleration profile, Gaussian function, motion dynamics, smooth jerk trajectory, vibration reduction.

I. INTRODUCTION

Industrial equipment, such as robots and computer numerical control (CNC) machines, carries out many distinct movements in a wide range of applications that require high speed, precision, and motion stability to maintain product quality keeping down production time and cost. Therefore, industrial equipment usually works at its limits, causing excessive long-term vibrations that worsen their movement stability and precision. This issue has attracted researchers attention, who have proposed a variety of strategies in literature, mainly focusing on the design and implementation of control laws or the proposal of reference motion profiles. The former has been widely studied [1], [2]; however, the latter is an open subject for new suggestions that allow diminishing the long-term vibration effects by manipulating the industrial-machine motion dynamics through the definition of templates for movement trajectories [3].

A machine motion dynamics is defined by its position, velocity, acceleration, and jerk profiles [4], [5], [6], [7]. It is well known that high jerk values produce high amplitude vibrations in a machine component. This has motivated researchers to look for new control approaches to limit jerk effects by producing smooth motion profiles [8], [9], [10]. The trapezoidal velocity profile is the most-common movement scheme applied to industrial machines [11], [12].

The associate editor coordinating the review of this manuscript and approving it for publication was Shihong Ding.

It consists of sudden acceleration changes that involve very high amplitude jerk. In recent approaches, researchers have proposed different motion profiles that alleviate some of the trapezoidal-speed-scheme issues by utilizing a variety of motion references like the one known as the S curve profile, which requires 3rd-degree polynomial functions for obtaining a smooth jerk pattern [13], [14], [15], [16]. This is achieved by making the start and the end of the reference scheme uniform. A smooth jerk profile brings physical and mechanical benefits to motors, as described in [17], where a trajectory, based on a defined jerk track and exponential-function filters, is proposed for reducing motion-system vibrations. A control system, which decreases undesirable output-force ripples using jerk minimization as the base model for obtaining a velocity profile by implementing a 5th-degree polynomial, is proposed in [18]. In [19], a trigonometric function is used for obtaining smooth acceleration and jerk profiles. An analytical algorithm is introduced in [20] for continuous corner smoothing during CNC machining. This approach is aimed to reduce jerk effects and decrease trajectory errors by obtaining a smoother piece. The look-ahead window technique is used in [21] and [22] for smoothing the path-geometry corners to reduce the jerk magnitude in a CNC machine through the jerk-limited acceleration profile, which consists of three phases: acceleration increment at continuous rate, followed by a constant acceleration, and a final deceleration at a sustained ratio. In [23], a method for characterizing a machine-tool trajectory movement is proposed based on the analysis and manipulation of velocity, acceleration, and jerk profiles. The approach is used for improving the manufacturing-process efficacy and productivity by lessening consumed resources as materials and energy during iterative machining tests; however, some discontinuities are noticed in the acceleration profile. A study in the movement trajectory of a robot is introduced in [24] based on an S-shaped acceleration and deceleration algorithm that employs complex polynomial functions for its implementation. The approach yields a smooth velocity curve reducing the execution time and guaranteeing soft movements in industrial robots. From the described above, it can be inferred that motion-profile implementation for industrial machinery has become a notorious subject in recent years. For instance, performance comparison and evaluation among four motion profiles are performed in [25] by assessing vibration decreasing and machine wear. The studied profiles are applied in a gripper arm and its drive train. In [26], the implementation and performance of different motion profiles are compared in a linear platform, with a flexible beam system used for verifying obtained results from a theoretical analysis. From reviewed literature, it is clear that a machine motion dynamics is improved by lessening jerk effects; unfortunately, 3rd- or higher-degree polynomial functions must be implemented in order to reach this outcome, making difficult their integration because of their computational complexity and high resources demand; furthermore, there are some trajectory discontinuities in the obtained profiles that provoke high jerk effects.

As mentioned previously, a smooth jerk profile in the motion dynamics allows reducing vibrations and possible damages in an industrial machine, as well as improving its movement precision and performance. Therefore, in this paper, an innovative acceleration profile based on a Gaussian function is proposed. This scheme is used for generating the position-reference outline to achieve a smooth motion trajectory of industrial machines. A jerk contour with smooth and continuous behavior is accomplished by using the Gaussian function as a basis to build the acceleration profile, from the desired values for maximum position, velocity, and acceleration, together with the estimation of all remainder-parameter outlines, which define the machine motion dynamics.

The remainder of the document is organized as follows: Section II presents the design of the proposed acceleration profile based on the suggested Gaussian function scheme. Section III describes the computer-based simulation and real-time experimentation carried out, as well as the results obtained from each treated case of study, and their contrast against the state of the art in the subject. Section IV provides some conclusions.

II. MATHEMATICAL FRAMEWORK

This section describes the mathematical fundament for the proposed Gaussian acceleration profile by defining motion dynamics, the Gaussian function behavior and its implementation as acceleration profile for motion dynamics reconstruction.

A. MOTION DYNAMICS

Motion dynamics has an essential impact on the design of displacement trajectories since it provides smoothness and precision during industrial equipment operation. Motion dynamics consist of consecutive derivative operations on a machine-movement function with respect to time, obtaining its corresponding mathematical expressions of speed, acceleration, and jerk. It is worth it to notice that motion dynamics can be obtained conversely by successive integration of the movement functions defining it. These expressions are known as motion dynamics profiles that delineate the corresponding position, velocity, acceleration, and jerk layouts. The relation among the distinct profiles, making up motion dynamics, is described from (1) to (3):

$$v(t) = \frac{d}{dt}p(t) \tag{1}$$

$$a(t) = \frac{d}{dt}v(t) \tag{2}$$

$$j(t) = \frac{d}{dt}a(t) \tag{3}$$

where $p(t)$, $a(t)$, $v(t)$, and $j(t)$ represent the position, velocity, acceleration, and jerk through time t, respectively.

B. GAUSSIAN FUNCTION

The Gaussian function in (4) is used for manipulating the acceleration profile to obtain smooth dynamics; hence,

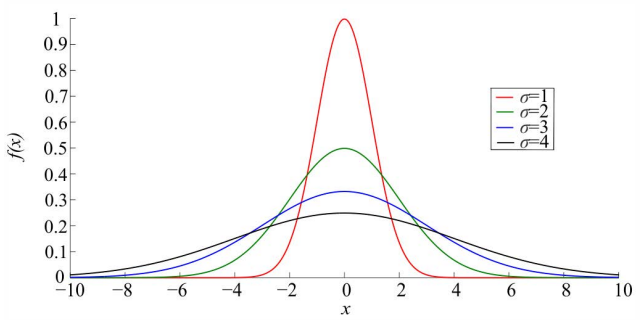

FIGURE 1. Gaussian function with different standard deviations.

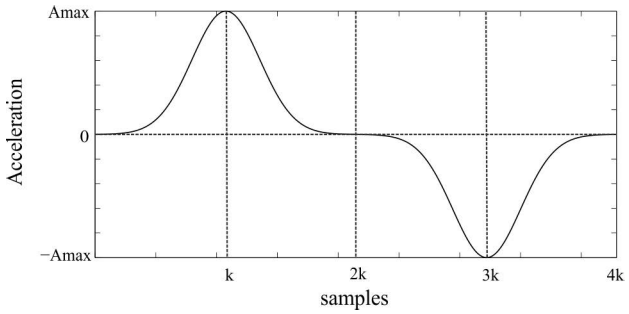

FIGURE 2. Proposed Gaussian acceleration profile.

the Gaussian function amplitude and width can be modified by adjusting the standard deviation σ, as depicted in Fig. 1.

$$f(x) = \frac{1}{\sigma\sqrt{2\pi}} e^{-\frac{(x-\mu)^2}{2\sigma}} \tag{4}$$

In (4), μ represents the mean of the discrete random variable x, and it can be used for shifting Gaussian bell in Fig. 1.

Therefore, different motion-dynamics parameters as position, velocity, and acceleration can be steered through a Gaussian function to obtain a smooth jerk pattern.

C. ACCELERATION PROFILE DESIGN

The proposed Gaussian acceleration profile produces a smooth machine movement that allows reducing vibrations and improving its motion precision, increasing the useful life of the machine mechanical parts. In this Gaussian layout, the maximum desired values for position (P_{max}), velocity (V_{max}) and acceleration (A_{max}), with corresponding units mm, mm/s and mm/s^2, are assumed. Therefore, the discrete values for these parameters are defined as follows, according to [27]:

$$P(n) = rp(t) \tag{5}$$

$$V(n) = \frac{r}{f_s} v(t) \tag{6}$$

$$A(n) = \frac{r}{f_s^2} a(t) \tag{7}$$

where n is the sample number, r is the ratio between the number of millimeters and the corresponding linear displacement generated in the machine, and f_s represents the sampling frequency.

The proposed Gaussian acceleration profile is divided into two segments, Gaussian acceleration, and Gaussian deceleration, each one of size $2k$ samples, as shown in Fig. 2.

The proposed acceleration profile starts with a 0 amplitude, and it reaches its maximum at the k-th sample; then, at the $2k$-th sample, the acceleration amplitude is zero again, reaching its minimum value at the $3k$-th sample. Finally, at the end of the proposed profile, the acceleration amplitude is 0 at the $4k$-th sample.

The discrete acceleration Gaussian profile is defined by (8).

$$A(n) = \begin{cases} A_{max} e^{-\frac{(\frac{n}{f_s}-k)^2}{2\sigma_{max}}} - d & 0 \le n < 2k \\ -A_{max} e^{-\frac{(\frac{n}{f_s}-3k)^2}{2\sigma_{max}}} + d & 2k \le n < 4k \end{cases} \tag{8}$$

From (8), it can be observed that the acceleration-profile amplitude is defined through its maximum value A_{max} scaled by an exponential, i.e., Gaussian, factor, plus an adjustment value d. (Please refer to Appendix IV for a thorough description).

The maximum standard deviation σ_{max} can be defined as a function of the maximum velocity and the maximum acceleration, as show in (9). (Please refer to Appendix IV for a thorough description).

$$\sigma_{max} = \frac{V_{max}}{A_{max}\sqrt{2\pi}} \tag{9}$$

The Gaussian-function double integral represents half of the maximum displacement in the motion dynamics, as described in (10). (Please refer to Appendix IV for a thorough description).

$$P(n) = (n-\mu)V(n) + \sigma^2 A(n) \tag{10}$$

In the $2k$-th sample of the proposed Gaussian profile, it is assumed that the machine has covered half of its maximum displacement, reaching its maximum velocity with an acceleration equal to zero at this point. Therefore, at the $2k$-th sample, the machine position is defined by (11).

$$\frac{P_{max}}{2} = (n-\mu)V_{max} \tag{11}$$

From (11), the function delay $(n–\mu)$ provides the value of k, so that, the acceleration profile starts with zero amplitude at sample zero, as defined in (12).

$$k = (n-\mu) = \frac{P_{max}}{2V_{max}} \tag{12}$$

Analyzing the proposed Gaussian acceleration-profile behavior, a discontinuity is observed at the junction of the acceleration and deceleration outlines; therefore, the adjustment value d is worked out by estimating k in (4), such

that the Gaussian acceleration-profile starts and ends with 0 amplitude, as defined in (13).

$$d = A_{max} e^{-\frac{(k)^2}{2\sigma_{max}}} \tag{13}$$

It should be noticed that to preserve the desired design parameters for the proposed acceleration profile, it would be necessary to use the maximum standard deviation defined in (9). If the used standard deviation value is selected within the range $0 < \sigma_{max}$, the maximum acceleration and jerk values increase, while the maximum velocity and position remain unchanged; under this condition the jerk profile remains smooth and continuous.

D. PROFILE RECONSTRUCTION

The profiles defining motion dynamics through the proposed acceleration profile are defined in (14) for reconstructing the jerk contour, in (15) for retrieving the velocity curve, and in (16) for recovering the controller position or reference outline.

$$J[n] = \frac{A[n] - A[n-1]}{f_s} \tag{14}$$

$$V[n] = \sum_{n=1}^{N} A[n] \tag{15}$$

$$P[n] = \sum_{n=1}^{N} V[n] \tag{16}$$

where N is the total number of samples. The motion dynamics profiles obtained through the proposed technique are depicted in Fig. 3, where the jerk profile shows a continuous and smooth behavior that guarantees the performance improvement of any motor or machine, obtaining additional benefits as system stability and precision by reducing vibrations in the motor or machine. Once the design parameters of the proposed Gaussian acceleration profile have been defined, the maximum value of jerk can be obtained by (17).

$$J_{max} = \frac{V_{max}}{\sigma^2\sqrt{2\pi}} e^{-\frac{1}{2}} \tag{17}$$

III. RESULTS

This section describes obtained motion-dynamics results from extensive software simulation, utilizing Matlab, and real-time experimentation. These results are compared and discussed against those from recent literature about the subject.

A. COMPUTER SIMULATION RESULTS

To demonstrate the smoothness and continuity of the jerk profile obtained through the introduced Gaussian acceleration outline, a computer-based modeling is carried out by modifying the design parameters described in Section II. Fig. 3 shows the determined shapes that define a machine motion dynamics when the introduced acceleration profile

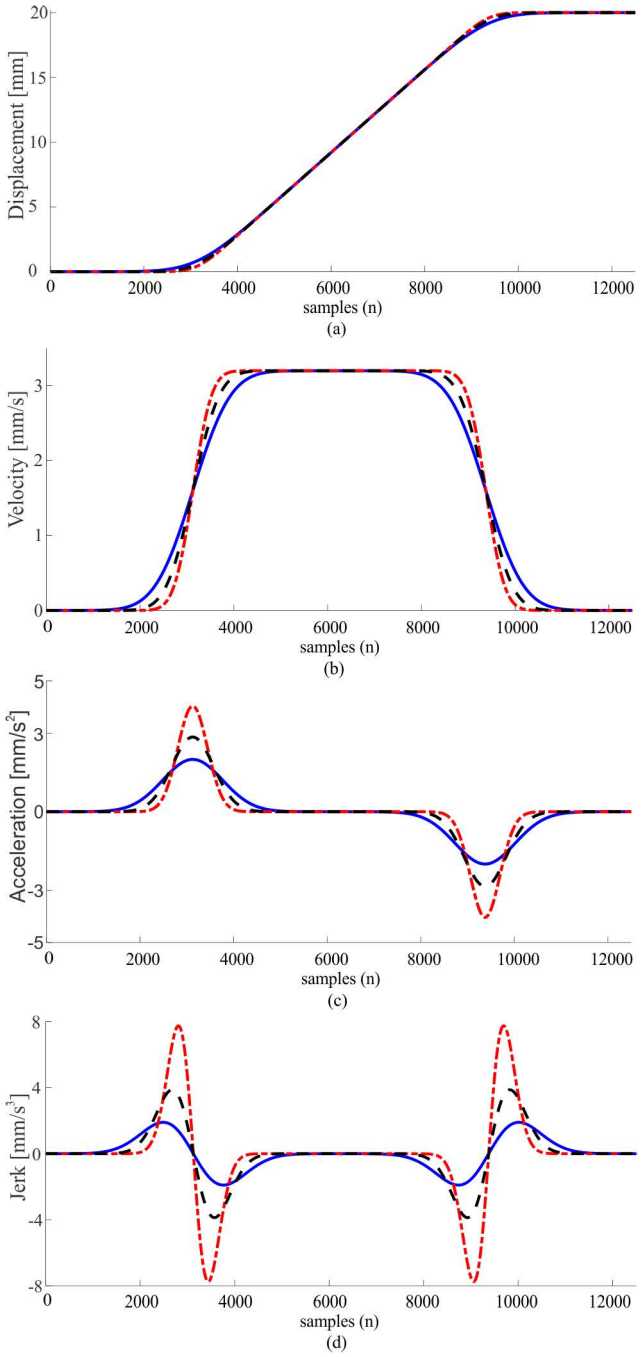

FIGURE 3. Profile simulation varying the standard deviation: $\sigma = 0.6383$ (maximum); $\sigma = 0.312$; $\sigma = 0.45$. (a) Position profile, (b) Velocity profile, (c) Acceleration profile, (d) Jerk profile.

is designed utilizing the following desired values: acceleration $= 2\ mm/s^2$, velocity $= 3.2\ mm/s$ and position $= 20mm$; hence, a $\sigma_{max} = 0.6383$ is obtained applying (9) that yields a maximum jerk peak of $1.9\ mm/s^3$. However, if the standard deviation (σ) is decreased, the acceleration and jerk profiles are modified; in both cases, the maximum peak values increase as shown in Fig. 3 (c) and Fig. 3 (d), but the maximum values obtained for the velocity and position

TABLE 1. Jerk comparison.

Profile	Maximum Jerk	Percentage
Trapezoidal Velocity	1.5109 x $10^6 mm/s^3$	100%
Trapezoidal Acceleration	4.0834 x $10^4 mm/s^3$	2.702%
Polynomial	4.0469 x $10^4 mm/s^3$	2.6784%
Proposed first derived form	1.7010 x $10^4 mm/s^3$	1.125%
Proposed second derived form	2.4260 x $10^4 mm/s^3$	1.605%

profiles are not changed, as depicted in Fig. 3 (b) and Fig. 3 (a), respectively. Similarly, if the standard deviation σ is decreased, the acceleration and jerk profiles are altered; in both cases, the maximum peak values increase, too, as shown in Fig. 3 (c) and Fig. 3 (d), but the top values obtained for the velocity and position profiles are continuous and smooth, without any alteration, as depicted in Fig. 3 (b) and Fig. 3 (a), respectively. Hence, if the standard deviation value is the maximum one that can be obtained utilizing the desired parameters; then, the minimum peak value of jerk will be produced.

On the other hand, if the desired position of the reference profile changes to 25 *mm* from 20 *mm*, and the maximum acceleration and maximum velocity are kept constant to 2 mm/s^2 and 3.2 mm/s, respectively, the maximum peak value of the jerk profile is sustained too. This is shown in Fig. 4; where, it can be seen that the velocity, acceleration, and jerk maximum peak value from their corresponding profiles are kept without change, as depicted in Fig. 4 (b), Fig. 4 (c), and Fig. 4 (d), respectively, and the jerk profile maintains a continuous and smooth shape. However, the execution time increases to achieve the desired position with these design parameters provided by the user.

The results obtained from the computer-based simulations demonstrate that a Gaussian acceleration profile designed through the proposed technique can regulate the motion-dynamics shapes by utilizing the configuration parameters defined in Section II, maintaining a continuous and smooth jerk profile over time, which will improve the performance of any industrial machine.

A depictive comparison against commonly used profiles in recent literature is performed to point up the effectiveness and improvement on a machine movement by utilizing the proposed approach. Fig. 5 contrasts the trapezoidal-velocity [12], [15], [26], [28], trapezoidal-acceleration [4], [5], [10], [13], [16], [17], [21], [22], [26], and polynomial profiles [3], [6], [9], [24], [25], [27], [28], against two associated variants of the proposed acceleration profile through computational simulation. The parameters for the first derived form of the proposed profile to carry out this comparison are: Displacement = 60 *mm*, maximum velocity = 198.8 mm/s, and maximum acceleration = 1500 mm/s^2. The second variant of the introduced profile changes the maximum speed to 246.4 mm/s and the maximum acceleration to 2000 mm/s^2 whereas the displacement remains to 60 *mm*.

From Fig. 5, it is evident the profile-behavior improvement by showing continuous and smooth paths with a remarkable

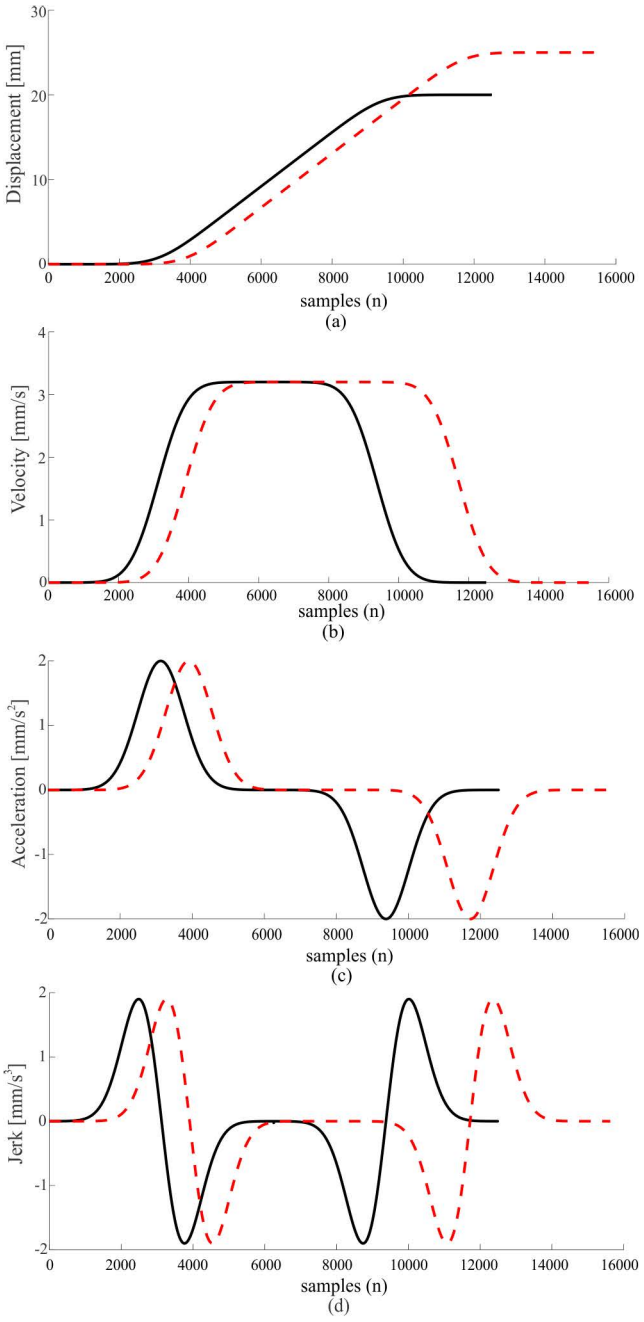

FIGURE 4. Profile simulation varying the reference position profile size: P= 25 mm; P= 20 mm (a) Position profile, (b) Velocity profile, (c) Acceleration profile, (d) Jerk profile.

maximum jerk reduction of more than 98% taking as reference that one from the trapezoidal-velocity profile. Table 1 shows the maximum jerk values from the commonly used profiles in literature and the two associated variants of the proposed acceleration profile. From this table it is worth it to notice that the first derived form of the proposed acceleration profile takes longer time than the others to reach its final displacement, but has the lowest maximum-jerk value; in contrast, the second variant of the proposed acceleration profile requires higher acceleration and velocity to keep the

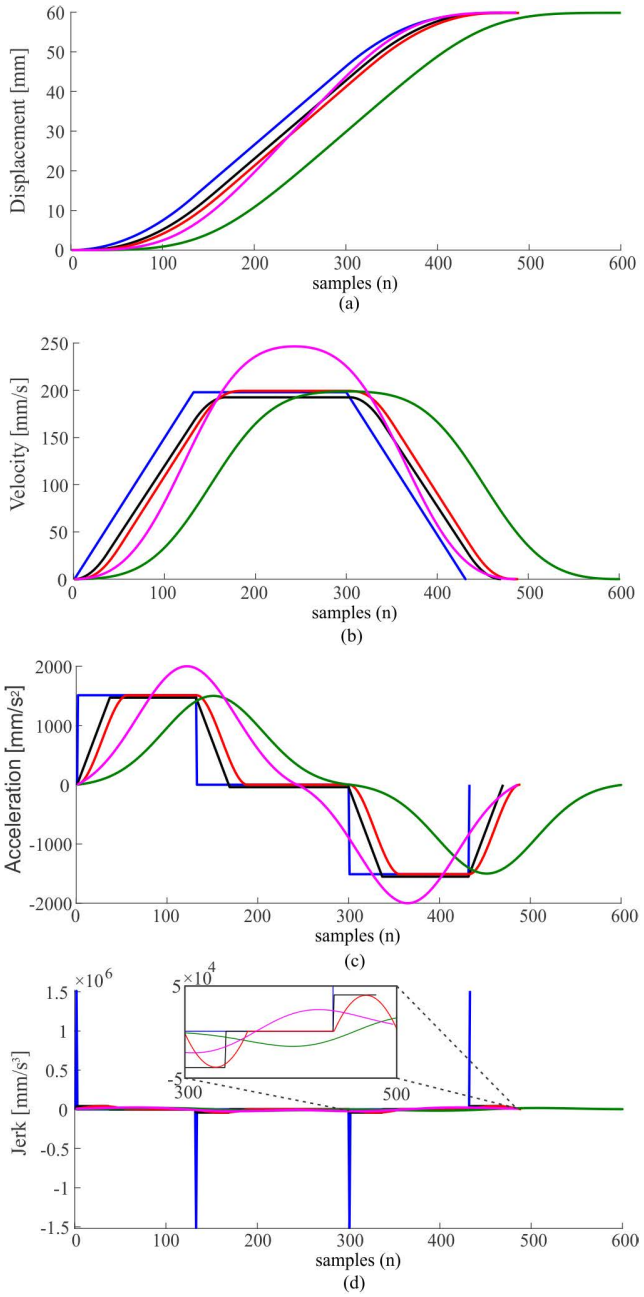

FIGURE 5. Profile-simulation comparison: Polynomial profile; Trapezoidal acceleration profile; Trapezoidal velocity profile; Proposed first derived form; Proposed second derived form; (a) Position profile, (b) Velocity profile, (c) Acceleration profile, (d) Jerk profile.

same execution, i.e. displacement, time than the commonly used profiles in literature, but still with a highly outstanding maximum jerk reduction.

The assessment of the presented approach was performed utilizing the software Matlab (R2020a) on a PC with an Intel Core i7-6500U microprocessor at 2.5 GHz, with 16 GB in RAM and a 64-bit operating system.

B. EXPERIMENTAL ASSESSMENT

The performance of the proposed technique is evaluated experimentally by designing an acceleration profile,

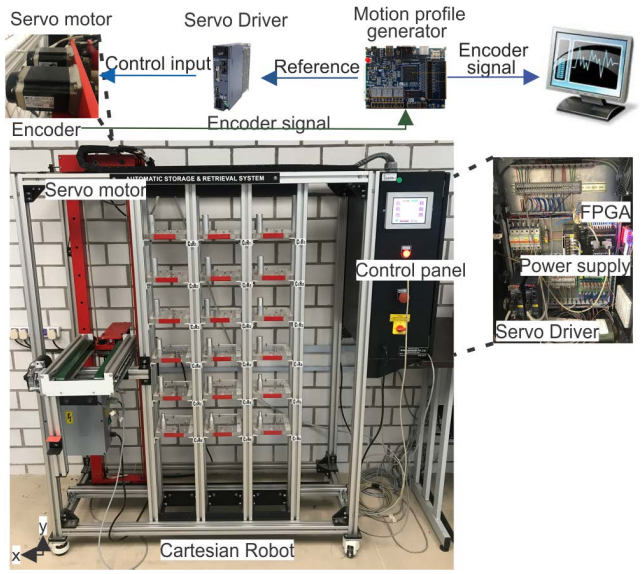

FIGURE 6. Experimental setup.

TABLE 2. Gaussian profile design parameters.

Parameters	First derived form	Second derived form	Max. Values Profiles
Position	60 mm	60 mm	60 mm
Velocity	198.8 mm/s	246.4 mm/s	198.8 mm/s
Acceleration	1500 mm/s^2	2000 mm/s^2	1500 mm/s^2
Standard deviation	0.003	0.003	-
Sampling frequency	1 KHz	1 KHz	1 KHz

according to the corresponding theoretical framework described in Section II of this work, for controlling the motion dynamics on the x-axis of a cartesian robot, which is a fundamental element of many production and industrial processes for carrying out high precision tasks.

The experimental setup is shown in Fig. 6 and consists of a servomotor (model GYB41D5-RC2), which has a 20-bit, serial encoder, a servo driver (RYH401F5-VV2), and a Terasic DE0-CV development board with an on-board Cyclone-IV field programmable gate array (FPGA) from Altera. The digital controller and the reference profile generator are embedded into the FPGA device.

Similarly to the computational simulation in the previous section, two variants of the proposed acceleration profile are used during the experimental validation utilizing the design parameters described in Table 2. The commonly used profiles in literature, i.e., trapezoidal-velocity, trapezoidal-acceleration, and polynomial profiles, are generated using the same configuration parameters as those in the first derived form of the proposed acceleration profile in Table 2, for comparison purposes. The obtained position profile (control reference) is sent to x-axis servomotor in the cartesian robot. Fig. 7 compares the displacement profile obtained from the experimental implementation of the commonly used profiles in literature and the first derived form for the proposed one. The experimentally computed profiles are obtained by

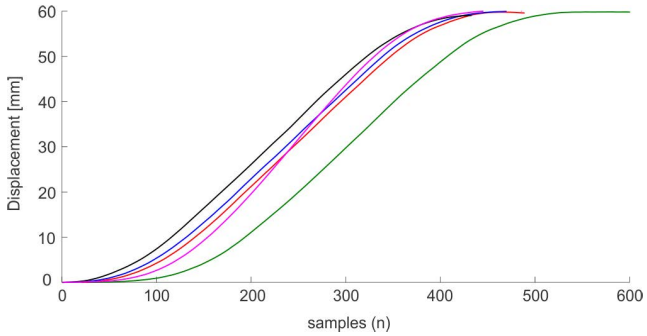

FIGURE 7. Experimental profiles comparison: Polynomial profile; Trapezoidal acceleration profile; Trapezoidal velocity profile; Proposed first derived form; Proposed second derived form.

TABLE 3. RMSE and jerk comparison of reference profile.

Profile	RMSE	Maximum Jerk
Trapezoidal Velocity	235.5 μm	8.31 x $10^4 mm/s^3$
Trapezoidal Acceleration	140.2 μm	7.8757 x $10^4 mm/s^3$
Polynomial	124.2 μm	6.98 x $10^4 mm/s^3$
Proposed first derived form	97.2 μm	4.821 x $10^4 mm/s^3$
Proposed second derived form	135.8 μm	5.4374 x $10^4 mm/s^3$

acquiring the position signal provided by the encoder and applying the estimation technique proposed in [28] to retrieve the system motion dynamics.

Table 3 shows the maximum jerk values and RMSE from all evaluated movement profiles.

C. DISCUSSION

The computer-based simulation of the proposed technique based on a Gaussian acceleration profile demonstrates that it is possible to handle the shape of the parameters that define a system motion dynamics through the maximum desired values of position, velocity and acceleration, maintaining a smooth and continuous jerk contour over time by taking into account the directives put forward in Section II. On the other hand, experimentally obtained results demonstrate that position can be tracked with a RMSE and maximum peak of jerk less than other commonly used motion profiles in literature, as described in Table 3; validating the high precision obtained by means of the proposed method, which, as described before, produces a smooth and continuous jerk profile.

From the results obtained through meticulous experimentations, it is clear that the first derived form of the proposed Gaussian acceleration profile produces a maximum jerk value of $4.821 \times 10^4 mm/s^3$, which is significantly lower than any other of the analyzed motion profiles. On the other hand, the second alternative form of the proposed Gaussian profile reaches a jerk peak value of $5.4374 \times 10^4 mm/s^3$, being just above the first configuration, but below all the commonly used motion profiles in literature, demonstrating the advantages of using the introduced strategy for diminishing the long-term vibration effects on motors or machines.

IV. CONCLUSION

High velocity, precision, and motion stability are required in industrial machines to maintain product quality and keep down production time and cost. Hence, a variety of schemes mainly based on the definition of control laws have been proposed for diminishing long-term vibration effects on industrial equipment. On the other hand, motion reference profiles have attracted researches interest in the recent years for tackling this issue by defining movement trajectories. Therefore, in this work, the design and implementation of a novel acceleration profile based on a Gaussian function is presented, which can be used for planning a robotic manipulator trajectory, and speed optimization in multi-axis industrial machines, such as lathes, CNC, and programmable universal machine for assembly, among many others. This strategy simplifies the position-profile estimation used as reference, and all-remainder parameters that define motion dynamics, producing a smooth and continuous jerk contour that reduces vibrations and improves the machine stability. On the other hand, by reducing the standard deviation for the Gaussian acceleration profile proposed in this work, the peak acceleration and jerk values increase, but the jerk outline remains smooth and continuous over time. Results obtained through exhaustive experimentation and comparison against commonly used profiles in literature show a remarkable lessening on the maximum jerk value of more than 98% taking as reference that one produced by the trapezoidal-velocity profile. Furthermore, computer-based simulations and real-time experimentation validate the proposed technique since a maximum jerk value of just $4.821 \times 10^3 mm/s^3$ and an RMSE on position profile of just 97.2 μm are obtained during the x-axis servomotor-trajectory tracking, outperforming all previously proposed approaches in the related subject.

Future Work: The proposed Gaussian acceleration profile will be implemented for assessing jerk effects on distinct industrial machines with multiple-axis trajectories.

APPENDIX A
GAUSSIAN FUNCTION FIRST INTEGRATION

Integrating (4)

$$\begin{aligned}
\int f(x) &= \int \frac{1}{\sigma\sqrt{2\pi}} e^{-\frac{(x-\mu)^2}{2\sigma^2}} dx \\
&= G \int e^{-\frac{(x-\mu)^2}{2\sigma^2}} dx \\
dx &= \sigma\sqrt{2} du \\
&= G \int e^{-u^2} \sigma\sqrt{2} du \frac{2\sqrt{\pi}}{2\sqrt{\pi}} \\
&= G\sigma\sqrt{\frac{\pi}{2}} \int \frac{2e^{-u^2}}{\sqrt{\pi}} \\
&= G\sigma\sqrt{\frac{\pi}{2}} (erf(u) + C) \\
&= G\sigma\sqrt{\frac{\pi}{2}} (erf(\frac{x-\mu}{\sigma\sqrt{2}}) + C) \qquad \text{(A.1)}
\end{aligned}$$

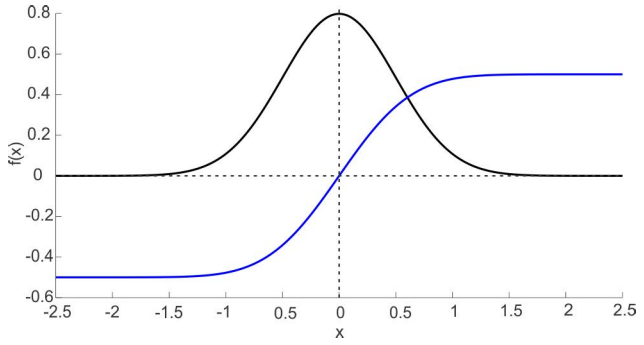

FIGURE 8. Gaussian function and integral.

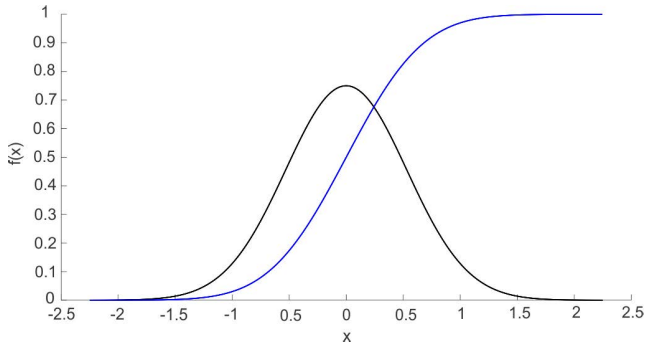

FIGURE 9. Gaussian function and integral with vertical displacement.

where G represents

$$G = \frac{1}{\sigma\sqrt{2\pi}} \tag{A.2}$$

The Fig. 8 shows the graphical representation of the Gaussian function with its integral

When $x = 0$ and $\mu = 0$ the maximum value of the Gaussian function is obtained, while in the integral half the maximum value of the function is obtained, therefore

$$\begin{aligned} f(0) &= G\sigma\sqrt{\frac{\pi}{2}}C \\ \frac{f_{max}}{2} &= G\sigma\sqrt{\frac{\pi}{2}}C \end{aligned} \tag{A.3}$$

Isolating C and sigma in (A.3) gives

$$\sigma = \frac{f_{max}}{CG\sqrt{2\pi}} \tag{A.4}$$

$$C = \frac{f_{max}}{G\sigma\sqrt{2\pi}} \tag{A.5}$$

Substituting (A.5) into (A.1)

$$\int f(x) = G\sigma\sqrt{\frac{\pi}{2}}(erf(\frac{x-\mu}{\sigma\sqrt{2}}) + \frac{f_{max}}{G\sigma\sqrt{2\pi}}) \tag{A.6}$$

and Fig. 9 shows the comparison of (4) and (A.6)

APPENDIX B
GAUSSIAN FUNCTION SECOND INTEGRATION

Taking and integrating (A.6)

$$\iint f(x) = \int G\sigma\sqrt{\frac{\pi}{2}}(erf(\frac{x-\mu}{\sigma\sqrt{2}}) + \frac{f_{max}}{G\sigma\sqrt{2\pi}}) \tag{B.1}$$

Changing of variable $p = x - \mu$ in (B.1) and takign (A.5)

$$\begin{aligned} \iint f(p) &= \int G\sigma\sqrt{\frac{\pi}{2}}(erf(\frac{p}{\sigma\sqrt{2}}) + C)dp \\ &= G\sigma\sqrt{\frac{\pi}{2}}(Cp + \int erf(\frac{p}{\sigma\sqrt{2}}) \\ u = \frac{p}{\sigma\sqrt{2}} \rightarrow du = \frac{1}{\sigma\sqrt{2}}dx \rightarrow dx &= \sigma\sqrt{2}du \\ &= G\sigma\sqrt{\frac{\pi}{2}}(Cp + \sigma\sqrt{2}\int erf(u)du) \end{aligned} \tag{B.2}$$

Solving the integral by parts gives

$$\begin{aligned} \iint f(p) &= G\sigma\sqrt{\frac{\pi}{2}}(Cp + \sigma\sqrt{2}(uerf(u) + \frac{1}{\sqrt{\pi}}e^{-u^2})) \\ &= G\sigma\sqrt{\frac{\pi}{2}}(Cp + \sigma\sqrt{2}((\frac{p}{\sigma\sqrt{2}})erf(\frac{p}{\sigma\sqrt{2}}) \\ &\quad + \frac{1}{\sqrt{\pi}}e^{-(\frac{p}{\sigma\sqrt{2}})^2})) \\ &= G\sigma\sqrt{\frac{\pi}{2}}(p)erf(\frac{p}{\sigma\sqrt{2}}) + \sigma^2 Ge^{-(\frac{p}{\sigma\sqrt{2}})^2} \\ &\quad + G\sigma\sqrt{\frac{\pi}{2}}Cp \\ &= G\sigma\sqrt{\frac{\pi}{2}}(x-\mu)erf(\frac{x-\mu}{\sigma\sqrt{2}}) + \sigma^2 Ge^{-(\frac{x-\mu}{\sigma\sqrt{2}})^2} \\ &\quad + G\sigma\sqrt{\frac{\pi}{2}}C(x-\mu) \end{aligned} \tag{B.3}$$

Factoring (B.3) and substituting (4) and (A.1) gives

$$\iint f(x) = (x-\mu)\int f(x) + \sigma^2 f(x) \tag{B.4}$$

REFERENCES

[1] D.-T. Nguyen, D. Saussie, and L. Saydy, "Design and experimental validation of robust self-scheduled fault-tolerant control laws for a multicopter UAV," *IEEE/ASME Trans. Mechatronics*, vol. 26, no. 5, pp. 2548–2557, Oct. 2021, doi: 10.1109/TMECH.2020.3042333.

[2] L. Guo, H. Chen, Q. Liu, and B. Gao, "A computationally efficient and hierarchical control strategy for velocity optimization of on-road vehicles," *IEEE Trans. Syst., Man, Cybern., Syst.*, vol. 49, no. 1, pp. 31–41, Jan. 2019, doi: 10.1109/TSMC.2018.2826005.

[3] K. K. Tan, X. Li, S.-L. Chen, C. S. Teo, and T. H. Lee, "Disturbance compensation by reference profile alteration with application to tray indexing," *IEEE Trans. Ind. Electron.*, vol. 66, no. 12, pp. 9406–9416, Dec. 2019, doi: 10.1109/TIE.2019.2892684.

[4] L. Biagiotti and C. Melchiorri, "Optimization of generalized S-curve trajectories for residual vibration suppression and compliance with kinematic bounds," *IEEE/ASME Trans. Mechatronics*, vol. 26, no. 5, pp. 2724–2734, Oct. 2021, doi: 10.1109/TIE.2018.2874617.

[5] W. Wang, C. Hu, K. Zhou, and S. He, "(B.6) corner trajectory smoothing with asymmetrical transition profile for CNC machine tools," *Int. J. Mach. Tools Manuf.*, vol. 144, Sep. 2019, Art. no. 103423, doi: 10.1016/j.ijmachtools.2019.05.007.

[6] A. Valente, S. Baraldo, and E. Carpanzano, "Smooth trajectory generation for industrial robots performing high precision assembly processes," *CIRP Ann.*, vol. 66, no. 1, pp. 17–20, 2017, doi: 10.1016/j.cirp.2017.04.105.
[7] M. Yuan, C. Manzie, M. Good, I. Shames, F. Keynejad, and T. Robinette, "Bounded error tracking control for contouring systems with end effector measurements," in *Proc. IEEE Int. Conf. Ind. Technol. (ICIT)*, Feb. 2019, pp. 66–71, doi: 10.1109/ICIT.2019.8755064.
[8] N. Kamaldin, S.-L. Chen, C. S. Teo, W. Lin, and K. K. Tan, "A novel adaptive jerk control with application to large workspace tracking on a flexure-linked dual-drive gantry," *IEEE Trans. Ind. Electron.*, vol. 66, no. 7, pp. 5353–5363, Jul. 2019, doi: 10.1109/TIE.2018.2870391.
[9] H. Ni, J. Yuan, S. Ji, C. Zhang, and T. Hu, "Feedrate scheduling of NURBS interpolation based on a novel jerk-continuous ACC/DEC algorithm," *IEEE Access*, vol. 6, pp. 66403–66417, 2018, doi: 10.1109/ACCESS.2018.2813334.
[10] P. Acharya, K.-D. Nguyen, H. M. La, D. Liu, and I.-M. Chen, "Non-prehensile manipulation: A trajectory-planning perspective," *IEEE/ASME Trans. Mechatronics*, vol. 26, no. 1, pp. 527–538, Feb. 2021, doi: 10.1109/TMECH.2020.3038591.
[11] L. A. Berardinis, "Motion control gets gradually better," *Mach. Des.*, vol. 66, no. 21, pp. 90–93, 1994.
[12] H. J. Yoon, S. Y. Chung, H. S. Kang, and M. J. Hwang, "Trapezoidal motion profile to suppress residual vibration of flexible object moved by robot," *Electronics*, vol. 8, no. 1, p. 30, Jan. 2019, doi: 10.3390/electronics8010030.
[13] Y. Liu, F. Liu, Y. Mei, and W. Wan, "Adaptive neural network vibration control for an output-tension-constrained axially moving belt system with input nonlinearity," *IEEE/ASME Trans. Mechatronics*, vol. 27, no. 2, pp. 656–665, Apr. 2022, doi: 10.1109/TMECH.2021.3126686.
[14] A. Dumanli and B. Sencer, "Data-driven iterative trajectory shaping for precision control of flexible feed drives," *IEEE/ASME Trans. Mechatronics*, vol. 26, no. 5, pp. 2735–2746, Oct. 2021, doi: 10.1109/TMECH.2020.3045444.
[15] P. A. S. Da Rocha, W. D. De Oliveira, and M. E. D. L. Tostes, "An embedded system-based snap constrained trajectory planning method for 3D motion systems," *IEEE Access*, vol. 7, pp. 125188–125204, 2019, doi: 10.1109/ACCESS.2019.2939116.
[16] Y. Bai, X. Chen, H. Sun, and Z. Yang, "Time-optimal freeform S-curve profile under positioning error and robustness constraints," *IEEE/ASME Trans. Mechatronics*, vol. 23, no. 4, pp. 1993–2003, Aug. 2018, doi: 10.1109/TMECH.2018.2835830.
[17] L. Biagiotti, C. Melchiorri, and L. Moriello, "Optimal trajectories for vibration reduction based on exponential filters," *IEEE Trans. Control Syst. Technol.*, vol. 24, no. 2, pp. 609–622, Mar. 2016, doi: 10.1109/TCST.2015.2460693.
[18] S. Masoudi, M. R. Feyzi, and M. B. B. Sharifian, "Force ripple and jerk minimisation in double sided linear switched reluctance motor used in elevator application," *IET Electric Power Appl.*, vol. 10, no. 6, pp. 508–516, Jul. 2016, doi: 10.1049/iet-epa.2015.0555.
[19] Y. Wang, D. Yang, R. Gai, S. Wang, and S. Sun, "Design of trigonometric velocity scheduling algorithm based on pre-interpolation and look-ahead interpolation," *Int. J. Mach. Tools Manuf.*, vol. 96, pp. 94–105, Sep. 2015, doi: 10.1016/j.ijmachtools.2015.06.009.
[20] J. Yang and A. Yuen, "An analytical local corner smoothing algorithm for five-axis CNC machining," *Int. J. Mach. Tools Manuf.*, vol. 123, pp. 22–35, Dec. 2017, doi: 10.1016/j.ijmachtools.2017.07.007.
[21] S. Tajima and B. Sencer, "Kinematic corner smoothing for high speed machine tools," *Int. J. Mach. Tools Manuf.*, vol. 108, pp. 27–43, Sep. 2016, doi: 10.1016/j.ijmachtools.2016.05.009.
[22] S. Tajima and B. Sencer, "Global tool-path smoothing for CNC machine tools with uninterrupted acceleration," *Int. J. Mach. Tools Manuf.*, vol. 121, pp. 81–95, Oct. 2017, doi: 10.1016/j.ijmachtools.2017.03.002.
[23] L. Chanda and R. J. Cripps, "Characterising the effects of shape on tool path motion," *Int. J. Mach. Tools Manuf.*, vol. 132, pp. 17–35, Sep. 2018, doi: 10.1016/j.ijmachtools.2018.04.005.
[24] S. Fang, J. Cao, Z. Zhang, Q. Zhang, and W. Cheng, "Study on high-speed and smooth transfer of robot motion trajectory based on modified S-shaped acceleration/deceleration algorithm," *IEEE Access*, vol. 8, pp. 199747–199758, 2020, doi: 10.1109/ACCESS.2020.3035430.
[25] W. Pawlus, M. R. Hansen, M. Choux, and G. Hovland, "Mitigation of fatigue damage and vibration severity of electric drivetrains by systematic selection of motion profiles," *IEEE/ASME Trans. Mechatronics*, vol. 21, no. 6, pp. 2870–2880, Dec. 2016, doi: 10.1109/TMECH.2016.2573587.
[26] C.-W. Ha and D. Lee, "Analysis of embedded prefilters in motion profiles," *IEEE Trans. Ind. Electron.*, vol. 65, no. 2, pp. 1481–1489, Feb. 2018, doi: 10.1109/TIE.2017.2726959.
[27] J. R. Rivera-Guillen, R. D. J. Romero-Troncoso, R. A. Osornio-Rios, A. Garcia-Perez, and G. Herrera-Ruiz, "Design methodology for fully dynamic-controlled polynomial profiles and reduced tracking error in CNC machines," *Int. J. Adv. Manuf. Technol.*, vol. 51, nos. 5–8, pp. 723–737, Apr. 2010, doi: 10.1007/s00170-010-2650-2.
[28] J. J. de Santiago-Pérez, R. A. Osornio-Rios, R. de J. Romero-Troncoso, G. Herrera-Ruiz, and M. Delgado-Rosas, "DSP algorithm for the extraction of dynamics parameters in CNC machine tool servomechanisms from an optical incremental encoder," *Int. J. Mach. Tools Manuf.*, vol. 23, no. 7, pp. 2383–2394, Oct. 2009, doi: 10.1016/j.ijmachtools.2008.06.004.

GONZALEZ-VILLAGOMEZ ESAU received the bachelor's degree in electronics engineering and the master's degree in applied electronics from the Department of Multidisciplinary Studies—Engineering Division of campus Irapuato—Salamanca, University of Guanajuato, Mexico, in 2017 and 2019, respectively, where he is currently pursuing the Ph.D. degree in engineering science. He received the distinction of "Recognition of Academic Merit" by the University of Guanajuato, in 2014 and 2018. His current research interests include embedded systems for real-time application, instrumentation, robotics, control, and automation.

RODRIGUEZ-DONATE CARLOS (Member, IEEE) received the B.E. degree from the Technological Institute of Celaya, Guanajuato, Mexico, in 2007, the M.E. degree from the University of Guanajuato, Guanajuato, in 2008, and the Ph.D. degree from the Autonomous University of Queretaro, Queretaro, Mexico, in 2012. He was a Postdoctoral stay with the Complutense University of Madrid, Madrid, Spain, from 2013 to 2014. He is currently a National Researcher with the Consejo Nacional de Ciencia y Tecnología, Mexico. In 2014, he joined the Division de Ingenierias del Campus Irapuato–Salamanca, University of Guanajuato, where he is an Associate Professor. His current research interests include digital signal processing, FPGAs, embedded systems for real-time application, instrumentation, control, and automation.

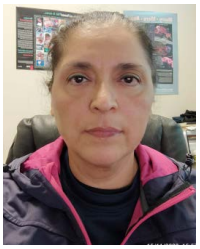

MATA-CHAVEZ RUTH IVONNE received the bachelor's degree in electronics engineering and the master's degree in electrical engineering from the FIMEE, University of Guanajuato, Salamanca, Guanajuato, Mexico, in 2000 and 2005, respectively, and the Ph.D. degree in science (optics) from the Optics Research Center, León, Guanajuato, in 2008. She is currently working with the University of Guanajuato as a Professor in the Engineering Division Campus Salamanca-Irapuato. Her current research interests include electronic and optical sensors, optical fiber devices, and optoelectronics.

CABAL-YEPEZ EDUARDO (Member, IEEE) received the B.Eng. and M.Eng. degrees from the Facultad de Ingenieria Mecanica Electrica y Electronica (FIMEE), Universidad de Guanajuato, Mexico, in 1999 and 2001, respectively, and the Ph.D. degree from the University of Sussex, U.K., in 2007. In April 2008, he joined the Division de Ingenierias, Campus Irapuato-Salamanca, Universidad de Guanajuato, where he is a leading Professor at the Multidisciplinary Studies Department. He has been author/coauthor of more than 95 research papers published in scientific journals and in conference proceedings. His current research interests include digital instrumentation, digital image and signal processing, artificial intelligence, smart sensors, real-time processing, FPGAs, power quality, power electronics, and embedded systems. He is currently an Active Member of the IEEE Instrumentation and Measurement Society and the IEEE Industrial Electronics Society. He is also a member of the National System of Researchers, level 2, the National Council for Science and Technology (CONACYT), Mexico.

LOPEZ-HERNANDEZ JUAN MANUEL received the B.E. and M.E. degrees from the University of Guanajuato, Mexico, in 1998 and 2001, respectively, and the Ph.D. degree in medical informatics from the Institut National Polytechnique de Lorraine, France, in 2006. He is currently a Full Professor with the Division de Ingenierias del Campus Irapuato–Salamanca, University of Guanajuato. His current research interests include digital signal and image processing, computer vision, and instrumentation applications.

PALILLERO-SANDOVAL OMAR received the B.S. degree from the Instituto Nacional de Astrofísica, Óptica y Electrónica INAOE, Mexico, the M.S. degree in engineering electronics from the University of Guanajuato, Mexico, and the Ph.D. degree in optics science from INAOE. He was trained in optical design using phase-space optics. He is currently a Professor with the Center for Research in Engineering and Applied Science (CIICAp), Mexico. His current research interests include digital signal processing, digital image processing, applied optical imaging systems in spectral imaging, microscopy, and optoelectronic systems.